DEU FMD 27(81) (2025) 507-516

Dokuz Eylül Üniversitesi Mühendislik Fakültesi Fen ve Mühendislik Dergisi
Dokuz Eylul University Faculty of Engineering Journal of Science and Engineering
Elektronik/Online ISSN: 2547-958X

RESEARCH ARTICLE / ARAŞTIRMA MAKALESI

Effect of Thickness Reduction in BIW Weight Reduction: Transition from 600DU to 800DU on Splitting Behavior

BIW Ağırlık Azaltmada Kalınlık Azaltımının Etkisi: 600DU'dan 800DU'ya Geçişin Yırtılma Davranışına Etkisi

Teoman Tilki, [1*], Yiğit Gönülalan [2], Onur Muratal [3], Diğdem Atabek [4]

[1,2,3,4] Toyotetsu Otomotiv Parçaları San. ve Tic. A.Ş, Kocaeli, Türkiye
Corresponding Author / Sorumlu Yazar *: tilkit@toyotetsu.com.tr, teomantilki@hotmail.com

Abstract

Material selection for creating a rigid and high-energy absorption lightweight BIW is critical in terms of fuel economy and emissions. In this context, material forming limits and mechanical behavior during stamping processes are the most important factors in the creation of lightweight BIW's. Therefore, enhancing strength and reducing material thickness stand out as the primary ways to comply with industry standards and reduce the body weight. In weight reduction efforts with dual-phase steels, thinning may lead to splitting due to the increased martensitic island structure in regions with the highest Mn and C content in dual-phase materials. In hot- and cold-rolled dual-phase 800DU material with a thickness of 1mm, splitting may occur during forming simulation due to the martensitic structure to distribute inhomogeneously, surpassing the critical threshold of the forming simulation curve when compared to cold-rolled 600DU material with a thickness of 1.2mm. This study addresses the thinning-induced splitting issue encountered in weight reduction applications, determining the optimal choice between different rolling types under a die produced for 600DU material with a thickness of 1.2mm, using both hot and cold-rolled materials. In line with the purpose of the study, trials were conducted with two different 800DU materials under forming dies. Formability simulations and mechanical tests were performed, and analyses were carried out in terms of microstructure, thinning, and edge cracking performance. The characterization of the materials was conducted using a scanning electron microscope (SEM) equipped with an EDX apparatus. Following the characterization, tensile tests were performed in three different rolling directions to determine the mechanical properties of the materials. To evaluate the resistance of the materials to edge cracking, Hole Expansion (HE) tests were conducted. As a result of the improvements and analyses made by replacing the 600DU material with a thickness of 1.2mm with cold-rolled 800DU material with a thickness of 1.0mm, the proposed application appears feasible for the part geometry under consideration.

Keywords: *BIW(Body-in-White) ,Weight Reduction, Dual Phases Steels, Necking, Edge Crack, Hole Expansion (HE)*

Öz

Rijit ve yüksek enerji emilimi sağlayan hafif Beyaz Gövde (BIW) yaratmak için malzeme seçimi, yakıt ekonomisi ve emisyonlar açısından kritik öneme sahiptir. Bu bağlamda, malzeme şekillendirme sınırları ve presleme işlemi sırasında mekanik davranış, hafif BIW oluşturmadaki en önemli faktördür. Bu nedenle, dayanımı yükseltmek ve malzeme kalınlığını azaltmak, endüstri standartlarına uyum sağlamak ve gövde ağırlığını azaltmanın birincil yolu olarak öne çıkmaktadır. Çift fazlı çeliklerde ağırlık azaltımı çalışmalarında incelme, çift fazlı çeliklerin içerdiği Mn ve C nedeniyle artan martensit adacık yapısının en fazla olduğu bölgeden yırtığa neden olabilmektedir. Sıcak ve soğuk haddelenmiş çift fazlı 800DU kalınlığı 1 mm olan malzemelerde, soğuk haddelenmiş 600DU kalınlığı 1,2 mm olan malzeme için yapılmış metal şekillendirme kalıbında martensit yapının homojen dağılamaması sebebiyle şekillendirme simülasyon eğrisinin kritik eşiğini aşarak yırtılma meydana gelebilir. Bu çalışmada, ağırlık azaltımı uygulamalarında karşılaşılan incelme kaynaklı yırtık problemi için sıcak ve soğuk haddelenmiş malzemeler ve 600DU, kalınlığı 1,2 mm olan sac için imal edilmiş kalıp altında farklı hadde türleri arasından optimum seçim belirlenmiştir. Çalışmanın amacı doğrultusunda, iki farklı 800DU sınıfı malzeme ile şekillendirme kalıbı altında deneme yapılmış; formabilite simülasyonları, mekanik testler gerçekleştirilmiş ve mikro yapı, incelme, kenar çatlama performansı açısından analiz edilmiştir. Malzemelerin karakterizasyonu, EDX aparatına sahip bir taramalı elektron mikroskobu (SEM) kullanılarak gerçekleştirilmiştir. Karakterizasyonun ardından, malzemelerin mekanik özelliklerini belirlemek amacıyla üç farklı haddeleme yönünde çekme testleri gerçekleştirilmiştir. Malzemelerin kenar çatlağına olan dirençlerini değerlendirmek amacıyla Delik Genişleme (HE) testleri uygulanmıştır. 600DU kalınlığı 1,2 mm olan malzemenin yerine 800DU soğuk haddelenmiş, kalınlığı 1,0 mm olan malzeme değişikliği yapılan iyileştirmeler ve analizler sonucunda uygulamanın yapıldığı parça geometrisinde mümkün gözükmektedir.

Anahtar Kelimeler: *BIW(Beyaz Gövde), Ağırlık Azaltımı, Çift Fazlı Çelikler, İncelme, Kenar Çatlağı, Delik Genişleme (DG)*

DOI: https://doi.org/10.21205/deufmd.2025278119

Geliş Tarihi / Received: 17.12.2024
Kabul Tarihi / Accepted: 26.03.2025

1. Introduction

More than ever, automotive industry have a strict limit for emissions, environmental demands and cost. Besides these strictions demand to automobile are increasing, customers expects more safer and fuel economy vehicles from industry. In this situation automobile manufacturers trying to provide more budget their R&D's for fulfill the strict limits and customer expectations. Automobile industry during their application considers reducing emissions and meanwhile providing the required performance of vehicles. These approaches can be summarized as follows: drive train efficiency improvement [1], development of new energy vehicles [2], alternative fuel systems [3] and vehicle weight reduction [4]. Among them, vehicle weight reduction has been considered as one of the most effective solutions and weight reduction of 57 kg is equivalent to 0.09–0.21 km per liter fuel economy increase. [5]

To achieve weight reduction improvement, the 600DU t=1.2mm material should be replaced with the 800DU t=1.0mm material. In order to achieve this improvement, factors influencing formability in DP materials have been taken into account.

Westhauser, Schneider and Denks, after hole expansion according to ISO 16630, Nakajima and tensile tests demonstrate that only a combination of high local strain and high fracture toughness leads to a high formability of punched edges. Prospectively, these two properties have to be taken into account individually for material characterization and future material development. [6]

Golovashchenko, Zhou and colleagues proposed, sheared edge stretchability measured in diffuse necking area and in hole expansion test illustrated that the best stretchability can be achieved for the cutting clearances 10…15% t. [7].

According to TOPSIS (Technique for Order of Preference by Similarity to Ideal Solution) method and GRA (Grey relational analysis) methods results show that the advanced high-strength steels are the optimal lightweight material for automobile applications. [8]

In order to obtain the goal of safe, lightweight, fuel efficient BIW one of the commercial car manufacturer floor side panel were choosed. Upgrading to material tensile strength 600DU to 800DU and reducing the material thickness 1,2mm to 1,0mm was evaluated from point of view thinning and edge crack performance. These subjects main reason for material choosing.

In this paper, reducing the weight of floor rear side panel at BIW %16. This calculation made it with given (Eq1).

Part Sheet Weight:

$$\text{sheet weight(g)} = \text{width} \times \text{pitch} \times \text{thickness} \times \text{specific gravity} \quad (1)$$

This paper aims, relationship between the thinning, edge crack and the stamping process parameters are established by press trial and as well as comparative analysis of two distinct 800DU grade material for BIW weight reduction applications.

Table 1. 600DU, XX1, XX2 Chemical Composition .wt %.

Element	C	Si	Mn	P	S	Al	Cu	Ti+Nb	B
600DU	0.15	0.75	2.5	0.040	0.015	0.015-1.5	0.20	0.15	0.005
XX1	0.18	0.8	2.5	0.050	0.010	1.0	0.15	0.15	0.005
XX2	0.18	0.80	2.5	0.050	0.010	1.0	0.20	0.15	0.005

2. Materials and Methods

The investigated part's choosing criteria were: i) should be from inside the safety cage ii) should be easily accessible on the vehicle body and iii) should not be something that is difficult or impossible to repair. Thus, the part chose to work on is one of the car manufacturers commercial vehicle floor rear side panels.

2.1. DP Steels Edge Fracture and Thinning

DP steels consist of a ferritic matrix containing a hard martensitic second phase in the form of islands, as shown in figure 1.

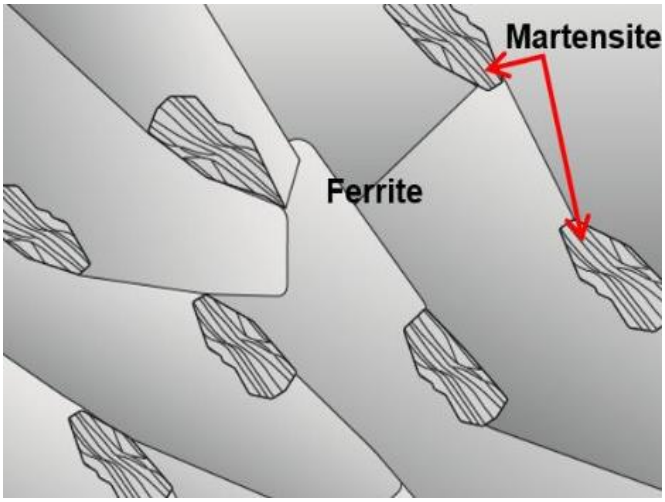

Figure 1. Island of martensite in a matrix of ferrite DP steel [9].

The soft ferrite phase is generally continuous, giving these steels excellent ductility.

During deformation of these steels, strain is concentrated in the lower-strength ferrite phase surrounding the islands of martensite, creating the unique high initial work-hardening rate (n-value) exhibited by these steels.[9]

Hot-rolled material, in the micrographs, martensite appears as darker regions surrounded by a lighter ferritic matrix. Pearlite is frequently observed in the microstructure of dual-phase steels. Its presence is generally undesirable due to its negative impact on cracking resistance during cold forming processes. The two critical temperatures in the strip cooling process, namely the intermediate coiling temp. and coiling temperatures, have a significant influence on the mechanical properties of DP steels. An increase in either of these temperatures leads to higher ultimate tensile strength (UTS) and reduced elongation [10].

Cold-rolled DP steels with a higher fraction of martensite exhibit increased strength due to the limited deformability of the martensitic phase. During the heat treatment process, the transformation from austenite to martensite occurs, resulting in volume expansion.

This transformation creates mobile dislocations around the martensite islands, which are located in the softer ferritic matrix in an unstrained state. The high dislocation density in the initial microstructure contributes to the continuous yielding behavior and a high initial work-hardening rate of DP steels. Additionally,

DP steels with a banded martensitic structure or large martensite islands tend to have lower elongation at fracture [11].

As shown in figure 2. the work hardening rate plus excellent elongation creates DP steels with much higher ultimate tensile strengths than conventional steels of similar yield strength.

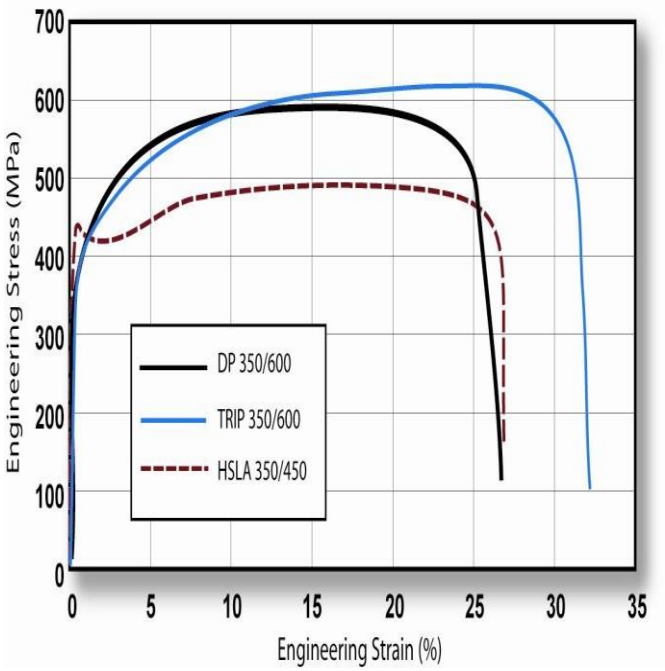

Figure 2. Stress strain curve for DP350/600[9].

Mukherjee, B. Bhattacharya [12] and colleagues revealed decreasing the difference in strength in constituent phases also contributes to a high hole expansion ratio,

L Pan, J. Xiong [13] and colleagues, reduced the difference in strength between the ferrite and martensite by adding Nb for increasing the strength of the soft ferrite matrix, and a satisfactory stretch-flangeability of the sheared edge was produced.

V. Balisetty and colleagues, suggested that the hole expansion ratio decreases with an increase in martensite content from 22 % to 45 % in the dual-phase (DP) steel [14].

Xu Sun and colleagues, ductile failure of dual phase steel was predicted when plastic strain localization occurred, which resulted from the inhomogeneous deformation concerning different hardnesses of the martensite phase and ferrite matrix [15].

Nguyen, Tong, conclude the effect of the burr orientation on the hole expansion ratio conclusion showed that the hole expansion ratio under burr down orientation is higher than that under burr up orientation [16].

2.2. Material and Chemical Composition

800DU cold rolled and 800DU hot rolled material commonly used in fields of automotive body in white manufacturing. In the present work we considered 600DU cold-rolled t=1,2mm, 800DU cold rolled and 800DU hot rolled steel sheet having a same tensile strength of 800DU. One of the material is hot rolled (XX2) one of them is cold rolled (XX1). Chemical composition of XX1 and XX2 are given table 1.

2.3. Forming Simulation

AutoForm simulation software is widely recognized as a powerful tool in the optimization of sheet metal forming processes, particularly within the automotive industry. By enabling virtual simulations of the entire stamping process, AutoForm allows for the prediction of material behavior during forming, which aids in identifying potential defects such as wrinkles, thinning, springback and edge crack.

The steps generated in the AutoForm simulation program and the input values are as shown in Figure 3.

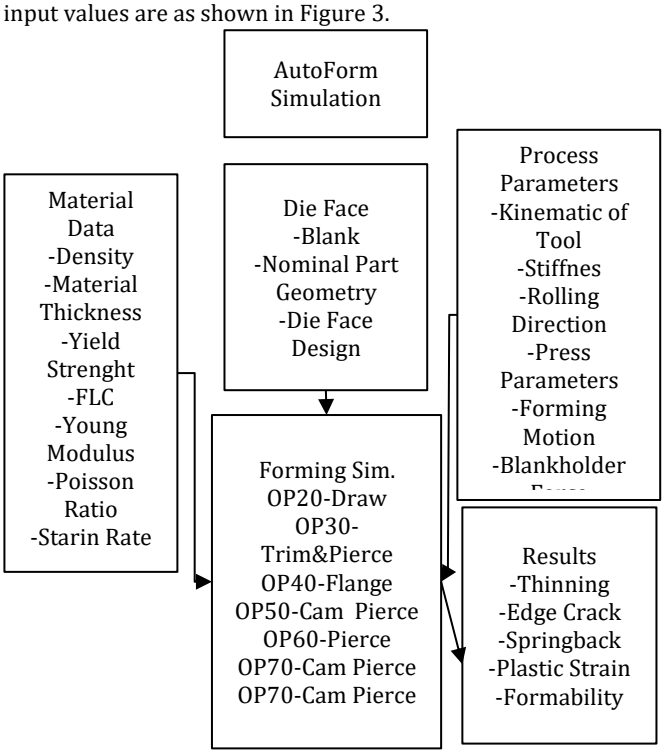

Figure 3. AutoForm created steps and data inputs scheme

Material card for CAE software provided from evaluated material manufacturer. Simulation card for XX1 material tensile strength 807,5MPa, yield strength 478MPa and strain hardening exponent(n)=0,168, XX2 material card, tensile strength 836,8MPa and yield strength of 510,6 MPa and strain hardening rate(n)=0,166. This values evaluated with mechanical tensile test and compared. As shown in figure 4. hardening curve, yield surface and FLC for 600DU t=1,2mm, 800DU t=1,0mm cold rolled and 800DU t=1,0mm hot rolled.

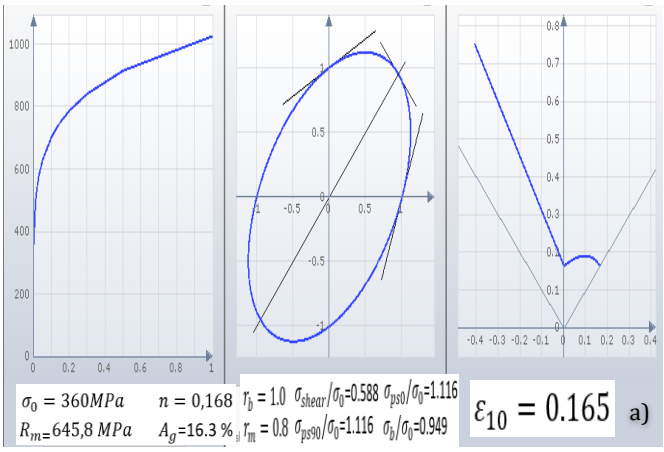

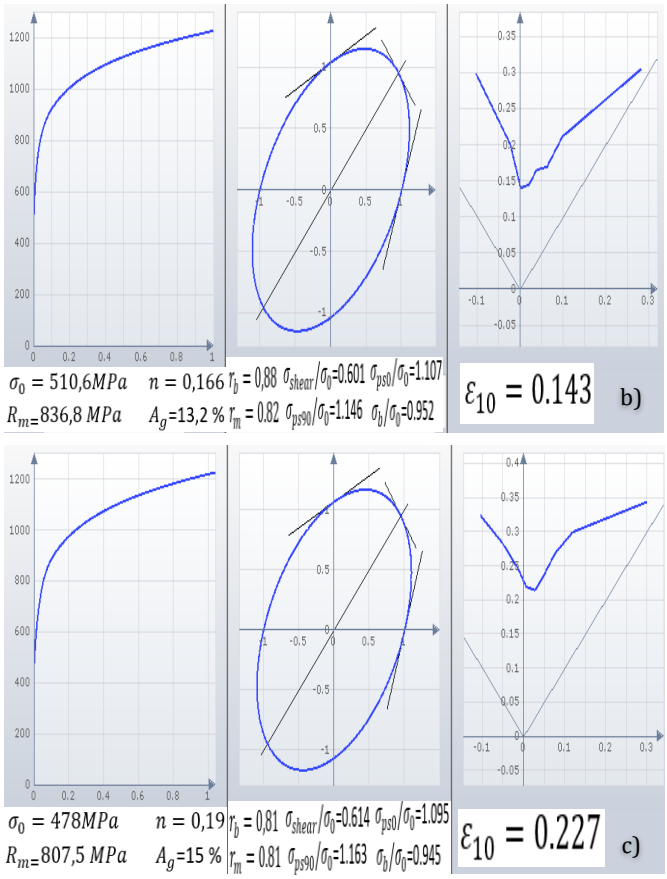

Figure 4. Hardening curve, yield surface and FLC (Forming Limit Curve) for a) 600DU t=1,2mm, b) 800DU cold rolled (XX1) t=1,0mm c) 800DU hot rolled (XX2) t=1,0mm

2.4. Preparation of Material for Metal Sheet Transfer Die

800DU cold rolled and 800DU hot rolled materials cutted from same blanking (cutting) die. Material cutting and shearing ratio is 1/3 cutting, 2/3 shearing of 1mm as shown in figure 5.

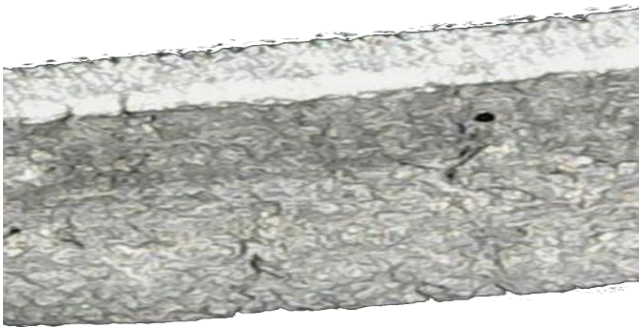

Figure 5. Cutting and shearing ratio, white brigh.t section-upper side cutting (1/3), rest is shearing (2/3) of 1mm.

Sheared materials evaluated by specified ratio. The blanking die employs a coil feeder for enhanced coil stability during the blanking (shearing) process, incorporating four side guides and four pilot pins. Cutting clearance is 15% of thickness [17]. Blanking press max. tonnage is 600ton. While cutting materials press machine operates at 40stroke/min for both of the material. Cutting speed calculated ≅ 2mm/sec given equation at 2. Die we use to stamp materials build one blank for one stroke.

$$v = \frac{s}{2}\omega 2\frac{22}{7}sin\alpha \qquad \text{(Eq2)}$$

s=press stroke, ω=angular frequency, α=press angle

J. Gu F. Alamos and colleagues believed that a high shearing speed contributes to an excellent local formability of the sheared edge by weighing the failure strain in the half specimen dome test (HSDT).[17]

2.5. Characterization of Microstructure

The samples were metallographically prepared with a Struers brand Tegramin 25 model automatic grinding and polishing device. Final polishing was performed on an MD Nap disc using a 1 µm suspension of DiaPro Nap B in water. Sample preparation processes were carried out in accordance with ASTM E3 standards. Between each metallography stage, the samples were dried in a Struers Lavamin brand automatic washing-drying device. After the metallography process, the samples were chemically etched with 4% nital solution. Microstructure images were obtained using a Nikon ECLIPSE MA 100 optical microscope and quantitative metallographic software (Clemex Vision Lite, Image Analysis Software 2.0C). Scanning electron microscope images were obtained on a ZEISS EVO-10 model instrument. The materials were subjected to a hardness test for 14 seconds under a load of 10 kg according to the TS EN ISO 6507-1 standard. Durascan 20 G5 model EMCOTEST brand hardness device was used in vickers hardness tests.

2.6. Tensile Test Specimens

To evaluate the edge fracture performance and thinning threshold, 800DU cold rolled material and 800DU hot rolled material mechanical test specimens were fabricated in accordance with JIS Z 2241 Tensile test method standards for metallic materials. Tensile specimens were cut from the sample die designed according to JIS. Rolling direction 0°, 45° and 90° Lo=50mm, Width=30mm mechanical test specimens were prepared as shown in Figure 6. Tensile tests of the prepared materials were conducted using a 5985 model INSTRON brand tensile testing apparatus.

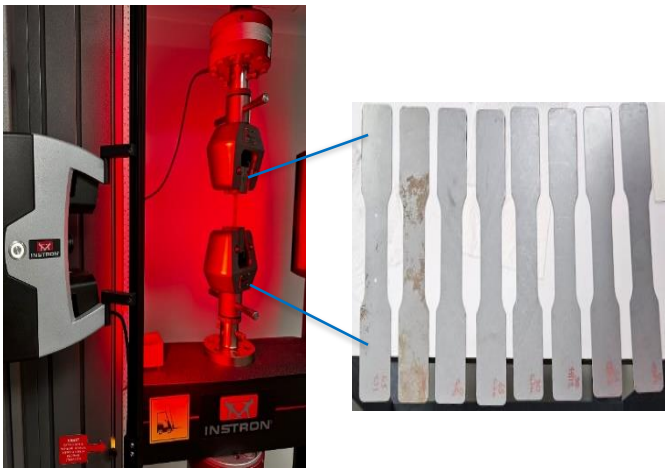

Figure 6. Tensile strength test apparatus and specimens according to JIS Z 2241 0°, 45°, 90° XX1, XX2.

2.7. HER Test Specimens

HER specimens prepared according to ISO16630. Test specimens of square shape were sheared from guillotine machine. Square specimen dimensions are 90x90mm. As shown in figure 7. punched hole cutted with HER specimen die at 1200t mechanical press. Cutting matrix is identical for both materials due to their thickness. Internal diameter of the die=10,30mm. Punch diameter is 10mm. Clearance applied between die and material is %15.

Figure 7. Specimen die for HER test.

2.8. Die Trial at 1600 Ton Eccentric Press

Press machine utilized for stamping 800DU cold rolled and 800DU hot rolled materials 1600ton A/C electric powered, eccentric gear transfer press, equipped with a finger-type unloading and transfer mechanism.

Prepared materials stamped under transfer metal sheet die as shown in figure 8. Stamping process includes draw process, trim & pierce process, flange process, cam & pierce process given process combined die has a total of 5 process. Distinct die operations amalgamated with 2 common plate. Each common plate contains 3 proses.

Stamping regulations for cold rolled and hot rolled material, draw process die cushion type is gas cylinder, lifter type at draw and flange process is spring-based. The force required for the flange procedure is specified by the formula in (Eq3).

$$P = c \times \delta_B \times L \times \frac{2t}{w} \quad (3)$$

c=coefficient, δ_B=tensile strength, L=bending length, t=thickness, w=shoulder width of die

Draw process required force calculated given formula at (Eq4).

$$F_U = \Pi.(d_1 + s).s.R_M.1{,}2.\ \frac{\beta-1}{\beta_{Max}}[N] \quad (4)[18]$$

d_1=punch diameter (mm), s=sheet thickness (mm), R_M=tensile strength (N/mm^2), β=draw ratio, β_{Max}=max. draw ratio

Closed die height parameter substituted with proportion to reduced thickness for overcome to springback (0,3mm).

OP20 is draw process. Cutted blanks to start with this process. Drawed t=1,0mm 800DU cold rolled and hot rolled 800DU material compared with 600DU t=1,2mm. OP30 trim&pierce process. In the drawing process, the extended sections added to prevent the metal sheet from slipping at draw process were cut from the metal sheet during OP30. The edge trimming and hole punching operations were performed within the same process. At OP40 flange operation applied to material.

3. Results and Discussion

3.1. Characterization of Microstructure

Figure 8. shows optical microscope images of 600DU and 800DU Dual Phase steels produced with two different techniques.

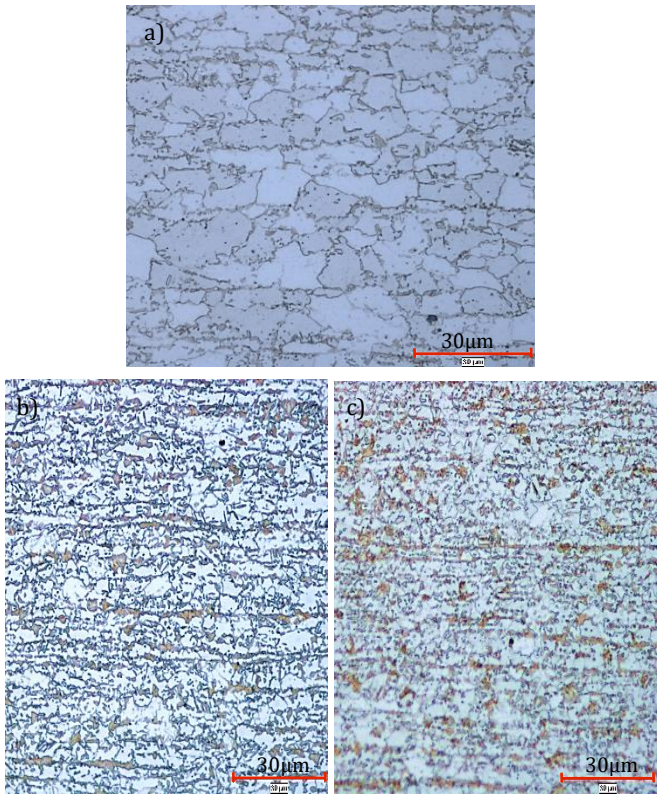

Figure 8. Optical microscope images of DP steels a) 600DU b) XX1 and c) XX2.

Upon examination of the microstructures, a characteristic dual-phase steel structure, consisting of fine ferrite grains with light contrast and martensite islands formed at ferrite grain boundaries with dark contrast is observed in 3 distinct materials. In Figures 20 b. and 20c., it is seen that martensite regions with dark contrast increase when the Mn ratio in the chemical composition escalates. Depending on the increasing Mn ratio in the chemical composition. It is observed that ferrite grains become thinner with increasing martensite ratio. Phase ratios resulting from differences in the chemical composition of steels used in the automotive industry affect their mechanical properties [19].

a)

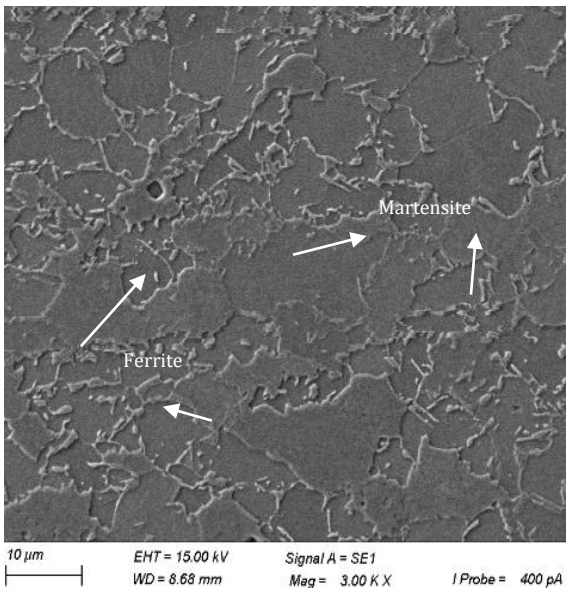

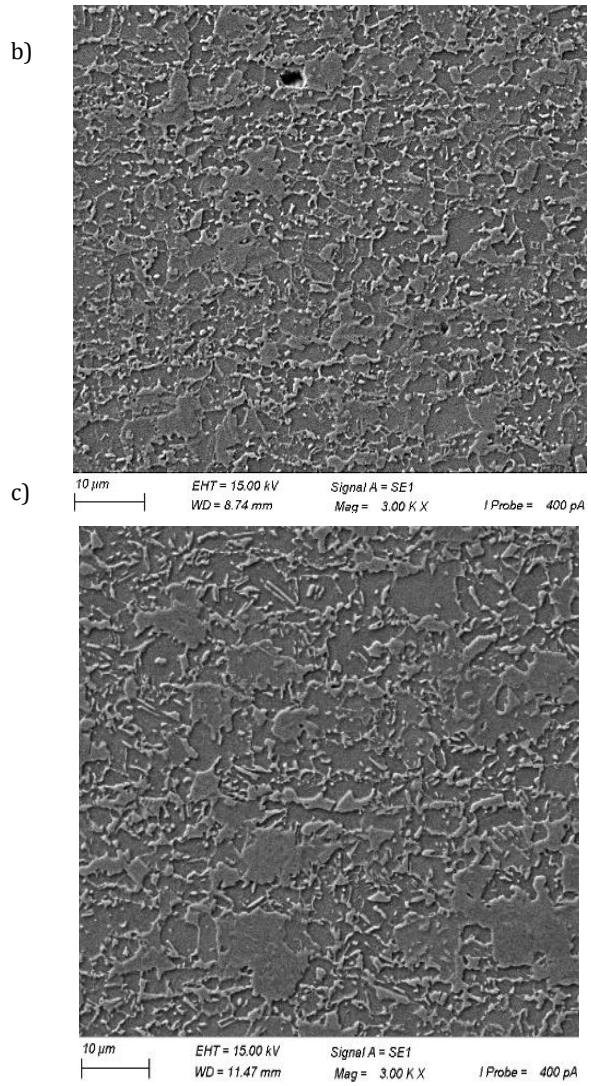

Figure 9. SEM microscope images of DP steels a) 600DU b) XX1 and c) XX2.

Upon examining the SEM images given in Figure 9. it is evident that the 600DU material given in Figure 9a exhibits coarser sized ferrite grains and less martensitic phase comparison to 800DU materials. In Figures 9b and 9c, the effects of two distinct production techniques on the microstructure are seen. It is seen that the XX1 cold rolled 800DU steel given in figure 9b. has a finer microstructure than the XX2 hot rolled steel given in 9c. Hot Rolled Steel the hot rolling process results in a coarser grain structure of the steel are influenced by rolling temperature. Cold rolling yields a finer and more consistent grain structure, resulting in enhanced strength, hardness, and other mechanical properties [20]. Section 3.1 elucidate the impact of microstructural alterations on mechanical characteristics.

3.2. Tensile and Hardness Test Results

The samples that fracture as a result of the tensile test tended to elongate and their width and thickness decreased visibly. This is a consequence of necking. Consequently, dual phase steels typically exhibit ductile fracture characteristics.

Tensile test graphs and results of standart 600DU, XX1 and XX2 coded samples depending on different rolling directions are given in Figure 10. and Table 2.

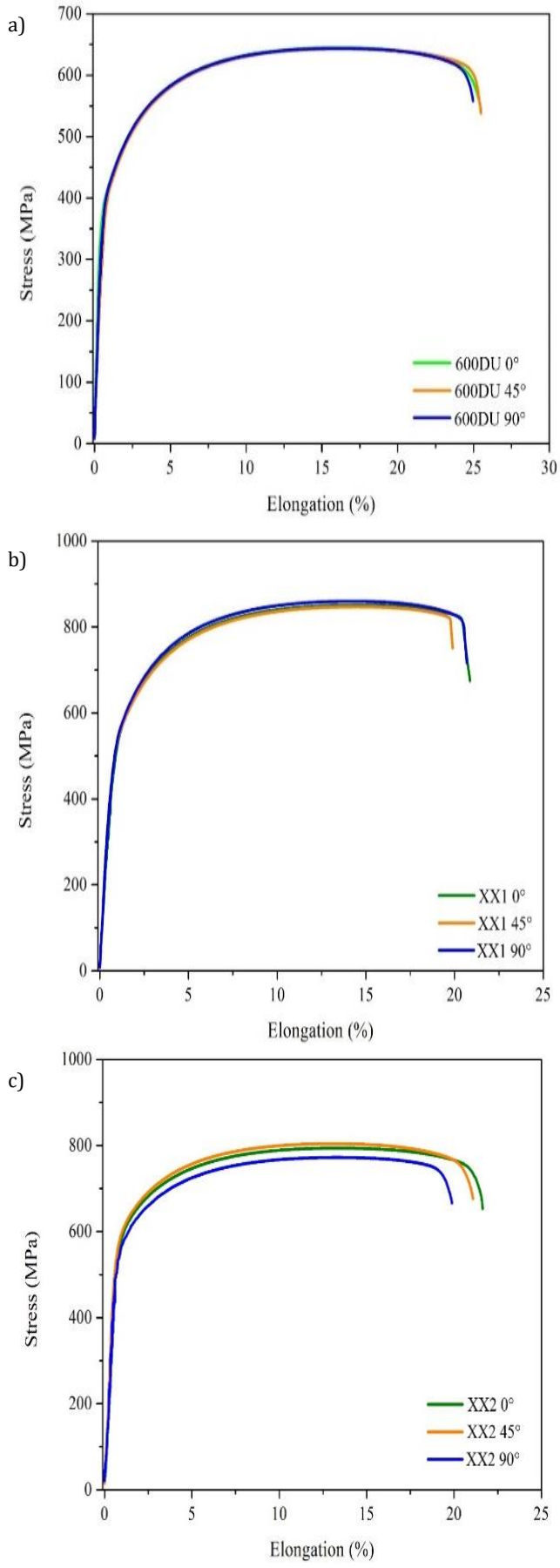

Figure 10. Stress – strain (%) graphs a) conventional 600DU b) XX1 and c) XX2 material in 0°, 45° and 90° directions.

Table 2. Tensile test results of XX1 and XX2 materials obtained at 0°, 45° and 90° rolling directions.

Samples	(Rp0.2) MPa	Elongation (%)	(Rm) MPa
XX1 0°	504,52	20,73	851,08
XX1 45°	488,30	20,17	847,18
XX1 90°	508,70	20,51	859,92
XX2 0°	563,52	21,53	794,17
XX245°	562,61	21,01	804,23
XX2 90°	545,06	19,81	772,40

When the tensile test results of 600DU steel with a thickness of 1.2 mm and 800DU steel are examined, the % elongation values of 600DU steel appear to be higher. This results from the elevated higher ferrite ratio in the matrix. The tensile test results of 800DU steels produced with two different techniques (cold rolled and hot rolled) were sufficient for part production despite the reduction in thickness. When the results of XX1 and XX2 steels with 800DU strength produced with two different techniques are examined, it is evident that the steel manufactured via cold rolling exhibits superior mechanical properties and a lower % elongation value due to a certain deformation hardening during the rolling process. This situation is directly affected by the annealing processes performed subsequent to cold rolling [21]. The annealing process directly affects the surface hardness of the materials. As shown in table3. this yields an increased hardness result of cold rolled steel [22].

Table 3. Hardness Test Results

Samples	Hardness (HV10)
XX1	261
XX2	228

3.3. HER Test Results

Comparative tests conducted on two distinct material for the floor rear side panel, as shown in figure 11 and figure 12. Commercially available hot rolled 800DU and other one will be commercially released soon 800DU cold rolled. Cold rolled specimens HER ratios shown in figure 11.

HER test conducted with Hole Expansion measurement system. Rolling direction at material aligned with machine specified direction. Hole 1/3 cutting ratio should be positioned at the conical punch side. The force applied is determined by the material thickness and grade as specified in table 2.

Hole expansion ratio HER, hole measured on basis of recorded pictures of camera. By setting six pixel points at the edge of the hole two isosceles triangles are defined, which are oriented perpendicular to each other to ensure an orthogonal measuring according to ISO 16330 [23].

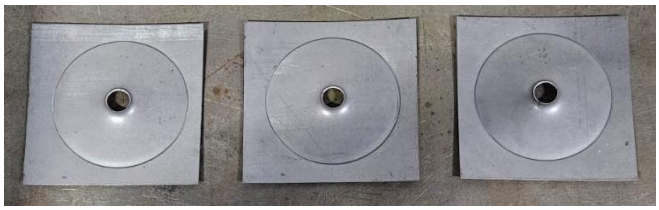

Figure 11. XX1, t=1,0mm HER specimens.

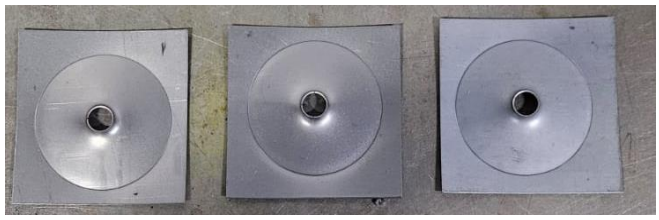

Figure 12. XX2 t=1,0mm HER specimens

Table 4. HER applied force chart (grade-thickness)

XXX	0,9mm	**1,0**	1,2	1,4	1,6	1,8	2,0	2,3
440-600	50kN	50	50	55	60	70	80	90
800	60	**60**	70	75	80	85	90	95

By the points 1-3 and 4-6 two measure circuits are defined, which diameters are the basis for the calculation of the averaged diameter of the hole D_h. In relation to standard specification the occurrence of first crack through the sheet thickness is the criteria for measuring the resulting diameter D_h. [24].

Determination of HER λ given at formula (Eq5).

$$\lambda = \frac{D_h - D_0}{D_h} . 100 \quad D_h = Initial, D_0 = \text{Final diameter.} \qquad \text{(Eq5.)}$$

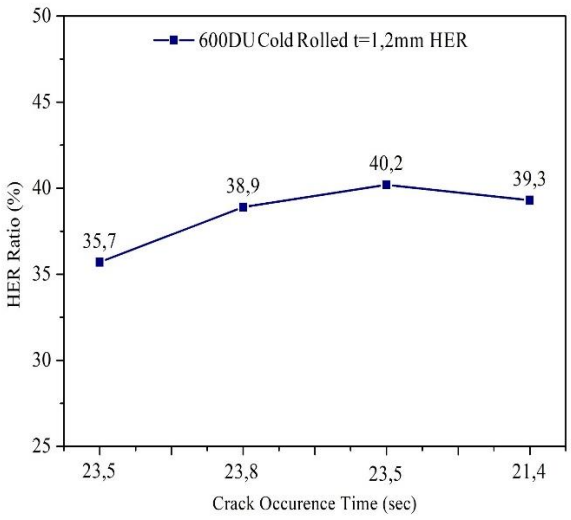

Figure 13. 600DU t=1,2mm HER-crack occurence time.

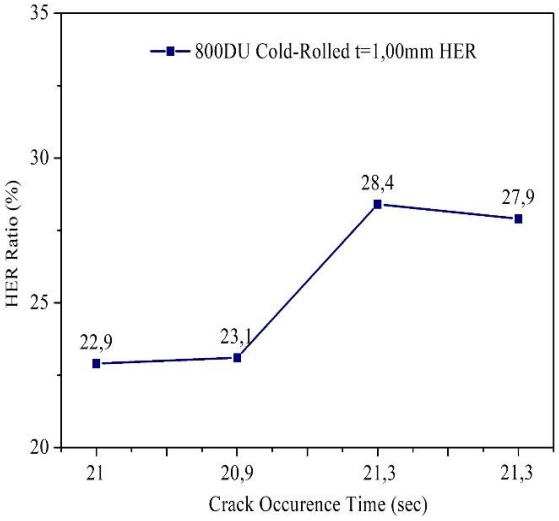

Figure 14. XX1 HER results.

As shown in figure 13. 600DU t=1,2mm material shows much higher HER than distinct XX1 and XX2. This result expected because as show in figure 9. 600DU material has much lower martensite C concentration compared to XX1 and XX2.

As shown in figure 13. 800DU cold rolled DU, exhibits edge cracks at a rate of %35 prior to hot rolled 800DU thus formability, edge crack and thinning performance on hot rolled 800DU is better. As shown in figure 14. specimens edge crack occurring time and specimens hole shape when analyzed 800DU cold rolled edge crack occurs ductile. Soft ferrite phase gives high ductility.

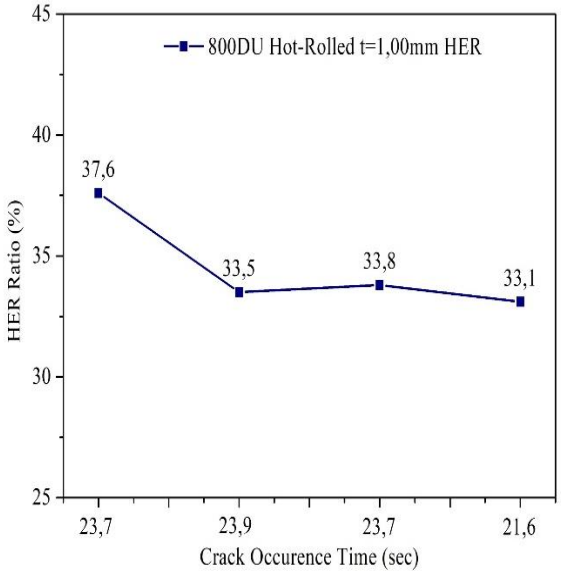

Figure 15. XX2 HER results.

As shown in figure 15. 800DU hot rolled HER exceeds the 800DU cold rolled. This disparity among the materials related with as shown in table 1. chemical composition cold rolled has a %wt 0,012 higher C contain. An increased martensite C concentration diminishes stretch-flangeability [25]. As shown in figure 15. the HER test findings for hot rolled material indicate more ductile expansion than cold rolled 800DU. The hole expansion ratio for XX2 is %35 superior than XX1 material.

3.4. Forming Simulation Results

As shown in figure 16. no edge cracking or split due to thinning was observed in the forming simulation of the part, which was aimed at reducing its weight.

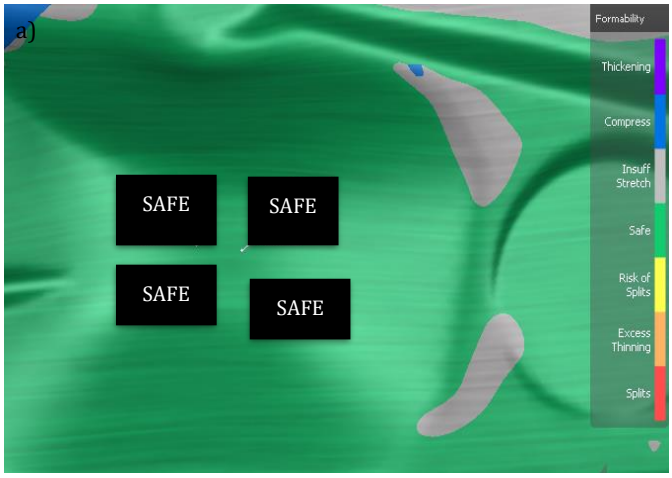

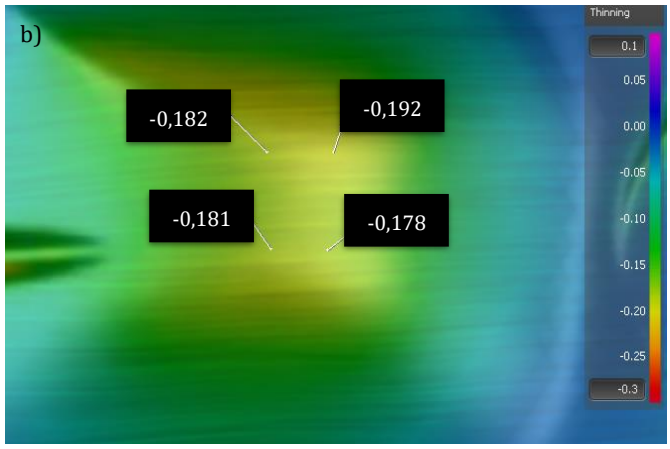

Figure 16. 600DU cold-rolled t=1,2mm forming simulation formability and thinning. a) formability, b) thinning (%).

In this study, according the simulation (figure 16, 17, 18) and die trial results is as shown in figure 20. concentrate to “dome”-like shape located in the lower center of the part.

As a result of the comparisons, it was observed that the 600DU t=1.2mm material has the highest formability without rupture in terms of thinning and split.

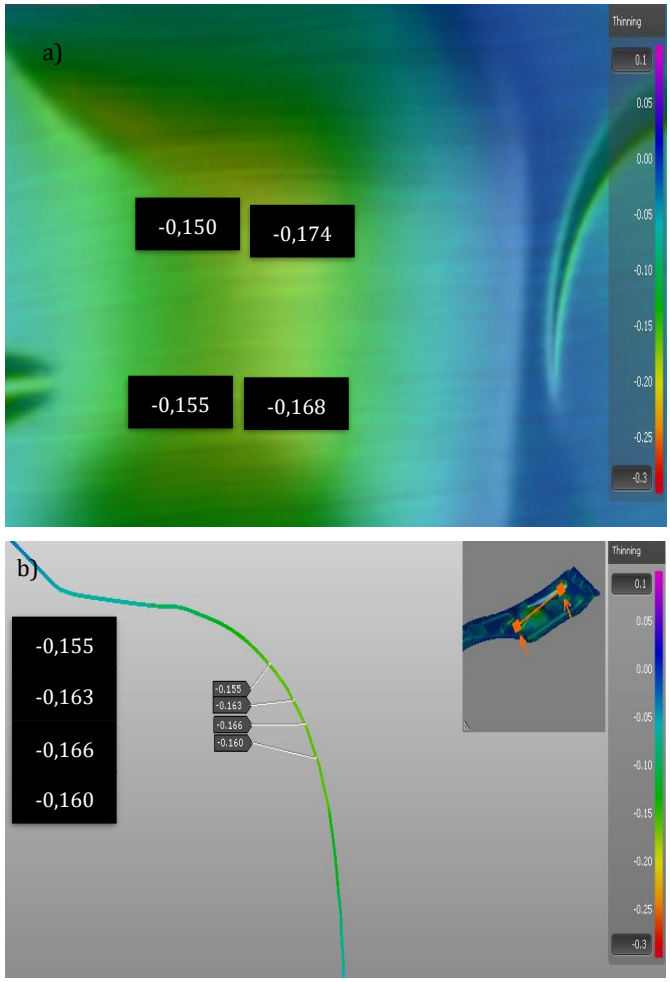

Figure 17. 800DU cold-rolled t=1,0mm forming simulation a) thinning (%), b) section of dome thinning.

In the simulation of the 800DU t=1.0mm cold-rolled material, thinning occurred. This comparison does not match the results obtained from the physical test conducted under the metal forming die. Cold-rolled (XX2) material in forming simulation show ≅17 thinning according to thickness. As shown in Figure 17, the simulation of the 800DU cold-rolled material exhibited thinning and subsequent rupture in areas close to the dome shaped mid-high region (figure 19).

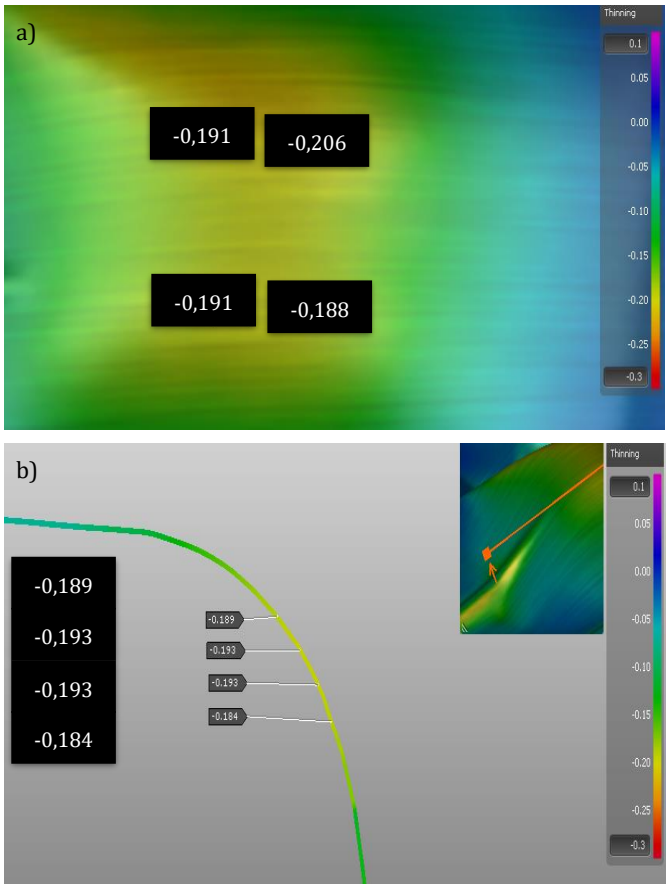

Figure 18. 800DU hot-Rolled t=1,0mm forming simulation a) thinning (%), b) section of dome thinning.

The hot-rolled 800DU t=1.0mm material showed better formability, closer to the 600DU t=1.2mm material. As shown in Figure 18, the simulation resulted in edge splitting due to thinning. This result does not match the findings from the physical test under the metal forming die (3.2.). Hot-rolled (XX2) material in forming simulation yield ≅20 thinning according to thickness of the material. This simulation results have ≅%2 higher than die trial thinning measurement (3.5.)

In terms of the formability, edge cracking due to thinning, which will affect weight reduction, the simulation results of the t=1.0mm 800DU hot-rolled and 800DU cold-rolled steels do not seem suitable to replace the 600DU t=1.2mm material for BIW weight reduction. As shown in Figures 17 and 18, the two different 800DU materials simulation results exceeded the critical minor and true strain safety thresholds, and rupture was observed.

3.5. Die Trial Results

In the metal forming die test, under section 3.4, the forming simulation results for thinning, splitting, and edge cracking highlighted the risky area, which, as shown in Figure 19, is focused on the "dome"-like shape located in the lower center of the part.

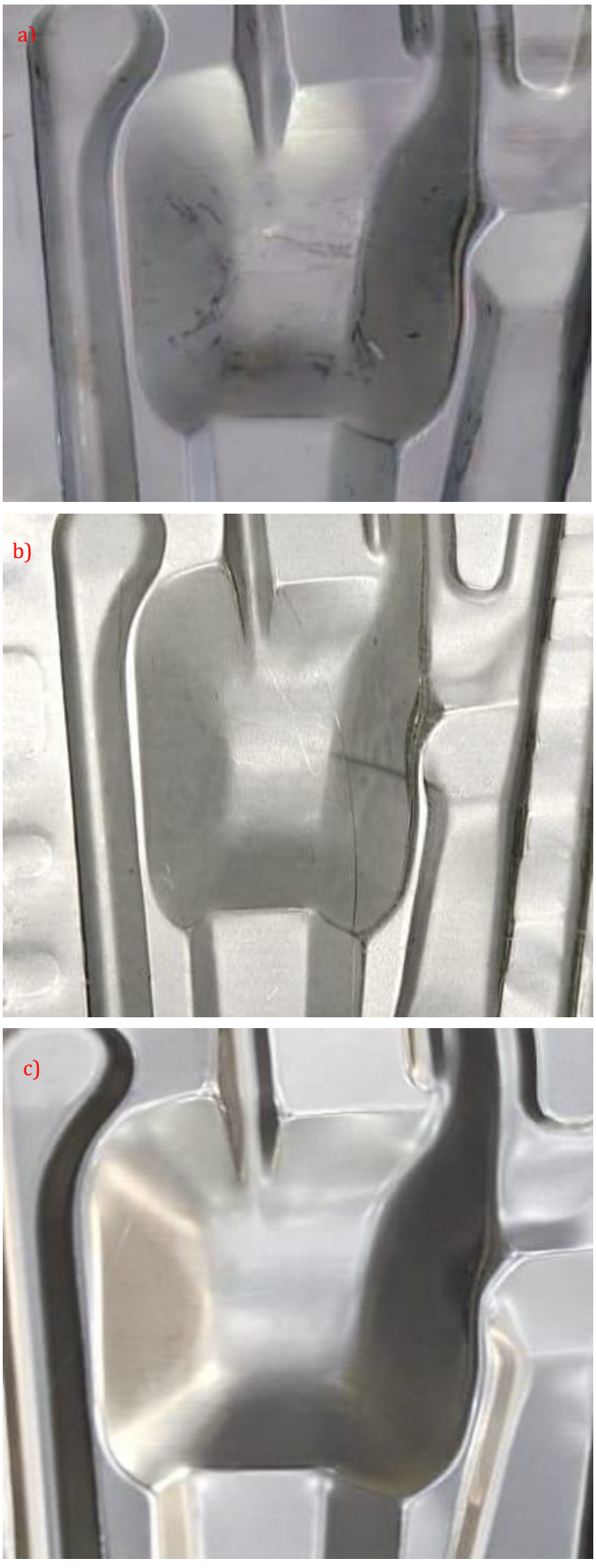

Figure 19. Drawn (OP20) panel comparison a) 600DU t=1,2mm, b) 800DU hot rolled t=1,0mm, c) 800DU cold rolled t=1,0mm.

As shown in figure 19. the visual comparison of the drawing process(OP20), which is paramount in terms of edge cracking and thinning, was made between 600DU t=1.2mm material, 800DU cold-rolled t=1.0mm and 800DU hot-rolled t=1.0mm materials. Issues such as wrinkling, edge cracking, and incomplete forming, which are expected to occur in the drawing process, have not been encountered. Thinning measurements conducted with Mitutoyo "External Digital Caliper Gauge". Thinning value calculated with given formula at (Eq6).

$$1 - \frac{Min.\ Measured\ Thickness}{Nominal\ Thickness} * 100 \qquad \text{(Eq6)}$$

Thinning values for 600DU cold rolled t=1,2mm %17, 800DU cold rolled t=1,0mm %18 and 800DU hot rolled t=1,0mm is %22. Selected part thinning tolerance for 1,0mm is %18. Thus, aspect of thinning cold-rolled 800DU t=1,0mm despite a thickness difference of 0.2mm, with welding and grinding intervention to OP20 and OP40 it remained within tolerance.

4. Conclusions

Dual Phase steels forming capability limited by edge crack, splitting caused by the shear cutting process and thinning under the sheet metal forming die, as shown in the test and forming simulation conducted above. Hard and ductile phases in Dual Phase steels creates very specific fracture mechanism due to void nucleation and coalescence mechanism. Although dual-phase materials meet all mechanical property requirements in tests, issues arise where they fail to achieve the minimum regional formability. This discrepancy is related to microstructure homogeneity, inclusion content, and edge conditions. Simulation programs can be misleading in this context as they do not account for these metallurgical characteristics. Therefore, when dealing with dual-phase materials, regional formability is assessed by producing the material under a metal forming die to observe the final result. Based on simulations, experimental die production, mechanical tests and microscope examinations, thinning, edge cracking and splitting in dual-phase steels is primarily influenced by the cutted edge condition, thinning, microstructure, particularly the strength and volume fraction of martensite.

In this study, the usability of hot or cold rolled 800DU steel with thinner thickness instead of the currently used 600DU steel within the scope of weight reduction studies was demonstrated. It is likely that when the martensitic phase reaches a critical volume fraction, there is a threshold for the damage energy associated with the microstructural damage at the two-phase interface.

a) In this study forming simulation conducted for cold-rolled 600DU t=1,2mm, 800DU t=1,0mm and hot rolled 800DU t=1,0mm materials. According to the forming simulation comparisons, the cold-rolled 800DU t=1.0mm material appears to be more suitable to replace the 600DU t=1.2mm material in the weight reduction application.
b) From quality aspect and according to die trial results 800DU cold rolled t=1,0mm material more close to mass production 600DU t=1,2mm. Nevertheless the die height was reduced in proportion to the decrease in thickness 0.3mm.
c) Due to factors such as the microscopic surface roughness or microstructural properties of the die surface, die wear, and die rigidity, which are either not considered or only partially considered by the forming simulation program, differences have been observed between the physical production (3.5.) and the simulation results (3.4.). Through forming simulation and die trial part springback condition welding and grinding interventions were applied to the die during the OP20 and OP40 processes.
d) Even the elongation difference avg=%0,31 of two distinct 800DU t=1,0mm material, edge cracking and thinning, which are influenced by the martensitic volume fraction and edge cut quality, were found to be improved in the cold-rolled 800DU material, which has a higher martensitic volume fraction and superior edge quality. As a result, this material exhibited better performance under sheet metal die in BIW weight reduction, making it the preferred choice.
e) Although according to die trial the cold-rolled 800DU t=1.0mm material yielded results closer to the nominal tolerances of the 600DU t=1.2mm material, it exhibited 0.3mm more springback behavior compared to the 800DU hot-rolled t=1.0mm material. As shown in Table 3, this issue is related to the fact that the hardness of XX1 material is 33% higher than that of XX2 material. The springback problem is associated with the tool, part geometry, and hardness. To eliminate the elastic recovery (springback) of the part, the die height was reduced by 0.3mm, and improvements as mentioned in article c) were implemented.
f) Cold-rolled DP steel (XX1), due to limited deformability of the martensitic phase showed increased strength. (Table3.) As shown in figure 9b. and figure14. due to banded martensitic structure yield lower elongation. Hot rolled DP steel (XX2), due to two critical temperature along with increasing, which is intermediate coiling temp. and coiling temp. lead to higher tensile strength and good formability.
g) Through forming simulation, die adjustments and material mechanic, visual tests, selected BIW part weight was reduced by 16%. A 100 kg weight reduction on BIW, fuel consumption will decrease by 0.6 L/100 km [26]. Thus 0,006 L/100km fuel saving achieved.
h) When examining the microstructure of the 800DU material produced by cold rolling, it has been observed that it exhibits a finer and more homogeneously distributed microstructure compared to the 600DU material produced by hot rolling. Microstructural analysis has demonstrated that cold-rolled steels exhibit a finer and more uniform structure than hot-rolled steels. Depending on the microstructural characteristics, it has been determined that the mechanical properties of cold-rolled steels are better.

References

[1] Manzie, C., Watson, H., Halgamuge, S. 2007. Fuel Economy Improvements for Urban Driving: Hybrid vs. Intelligent Vehicles, Transportation Research Part C: Emerging Technologies, Vol. 15, no. 1, pp. 1-16, DOI: 10.1016/j.trc.2006.11.003.
[2] Tian, G., Zhou, M., Li, P. 2017. Disassembly Sequence Planning Considering Fuzzy Component Quality and Varying Operational Cost, IEEE Transactions on Automation Science and Engineering, Vol. 15, no. 2, pp. 748-760, DOI: 10.1109/TASE.2017.2690802.
[3] MacLean, H.L., et al. 2000. A Life-Cycle Comparison of Alternative Automobile Fuels, Journal of the Air & Waste Management Association, Vol. 50, no. 10, pp. 1769-1779, DOI: 10.1080/10473289.2000.10464209.
[4] Helms, H., Lambrecht, U. 2007. The Potential Contribution of Light-Weighting to Reduce Transport Energy Consumption, International Journal of Life Cycle Assessment, Vol. 12, no. 1, pp. 58-64, DOI: 10.1065/lca2006.07.258.
[5] Han, H.N., Clark, J.P. 1995. Lifetime Costing of the Body-in-White: Steel vs. Aluminum, JOM, Vol. 47, pp. 22-28, DOI: 10.1007/BF03221171.
[6] Westhauser, S., Schneider, M., Denks, I.A. 2017. On the Relation of Local Formability and Edge Crack Sensitivity, International Conference on Steels in Cars and Trucks, June 18-22, Nordwijkerhout, Steel Institute VDEh.

[7] Nasheralahkami, S., Zhou, W., Golovashchenko, S. 2019. Study of Sheared Edge Formability of Ultra-High Strength DP980 Sheet Metal Blanks, Journal of Manufacturing Science and Engineering, Vol. 141, DOI: 10.1115/1.4044098.
[8] Zulqarnain, M., Dayan, F. 2017. Selection Of Best Alternative For An Automotive Company By Intuitionistic Fuzzy TOPSIS Method, International Journal of Scientific & Technology Research, Vol. 6, no. 10.
[9] Keeler, S., Kimchi, M., Mooney, P.J. Advanced High-Strength Steels Applications Guidelines Version 6.0. WorldAutoSteel.
[10] Kaźmierski, T., Krawczyk, J., Frocisz, Ł. 2023. Characteristic of DP600 steel Produced in Hot Rolling Process, Archives of Metallurgy and Materials, Vol. 68, no. 4, DOI: 10.24425/amm.2023.146234.
[11] Uthaisangsuk, V., Prahl, U., Bleck, W. 2011. Modelling of Damage and Failure in Multiphase High Strength DP and TRIP Steels, Engineering Fracture Mechanics, Vol. 78, no. 3, pp. 469-486, DOI: 10.1016/j.engfracmech.2010.08.017.
[12] Mukherjee, M., Tiwari, S., Bhattacharya, B. 2018. Evaluation of Factors Affecting the Edge Formability of Two Hot Rolled Multiphase Steels, International Journal of Minerals, Metallurgy, and Materials, Vol. 25, pp. 199-215, DOI: 10.1007/s12613-018-1563-1.
[13] Pan, L., Xiong, J., Zuo, Z., Tan, W., Wang, J., Yu, W. 2020. Study of the Stretch-Flangeability Improvement of Dual Phase Steel, Procedia Manufacturing, Vol. 50, pp. 761-764, DOI: 10.1016/j.promfg.2020.08.137.
[14] Balisetty, V., Chakkingal, U., Venugopal, S. 2021. Evaluation of Stretch Flangeability of Dual-Phase Steels by Hole Expansion Test, The International Journal of Advanced Manufacturing Technology, Vol. 114, pp. 205-217, DOI: 10.1007/s00170-021-06850-9.
[15] Sun, X., et al. 2009. Predicting Failure Modes and Ductility of Dual Phase Steels using Plastic Strain Localization, International Journal of Plasticity, Vol. 25, no. 10, pp. 1888-1909, DOI: 10.1016/j.ijplas.2008.12.012.
[16] Nguyen, D.-T., Tong, V.-C. 2021. A Numerical and Experimental Study on the Hold-Edge Conditions and Hole-Expansion Ratio of Hole-Blanking and Hole-Expansion Tests for Ferrite Bainite Steel (FB780) Sheets, Ironmaking & Steelmaking, Vol. 48, no. 8, pp. 986-994, DOI: 10.1080/03019233.2020.1849934.
[17] Gu, J., et al. 2020. A Study on Effects of the Press Speed on Sheared Edge Formability, IOP Conference Series: Materials Science and Engineering, Vol. 967, no. 1, p. 012064, DOI: 10.1088/1757-899X/967/1/012064.
[18] Lange, K. 1985. Handbook of Metal Forming. Third edition, McGraw-Hill, New York.
[19] Giray, D., Sönmez, M.Ş., Yamanoglu, R., Yavuz, H.I., Muratal, O. 2024. Characterization of Corrosion Products Formed in High-Strength Dual-Phase Steels Under an Accelerated Corrosion Test, Engineering Science and Technology, an International Journal, Vol. 57, p. 101796, DOI: 10.1016/j.jestch.2024.101796.
[20] Akpan, E.I., Haruna, I.A. 2012. Structural Evolution and Properties of Hot Rolled Steel Alloys, Journal of Minerals & Materials Characterization & Engineering, Vol. 11, no. 4, pp. 417-426.
[21] Ebrahimi, F., Saeidi, N., Raeissi, M. 2020. Microstructural Modifications of Dual-Phase Steels: An Overview of Recent Progress and Challenges, Steel Research International, Vol. 91, no. 10, p. 2000178.
[22] Kuang, S., Kang, Y.L., Yu, H., Liu, R.D. 2009. Effect of Continuous Annealing Parameters on the Mechanical Properties and Microstructures of a Cold Rolled Dual Phase Steel, International Journal of Minerals, Metallurgy and Materials, Vol. 16, no. 2, pp. 159-164.
[23] ISO 16630. 2009. Metallic Materials Method of Hole Expanding Test. International Organization for Standardization, Berlin: Beuth.
[24] Tsoupis, I., Merklein, M. 2016. Edge Crack Sensitivity of Lightweight Materials Under Different Load Conditions, IOP Conference Series: Materials Science and Engineering, Vol. 159, p. 012017, DOI: 10.1088/1757-899X/159/1/012017.
[25] Madrid, M., et al. 2018. Effects of Testing Method on Stretch-Flangeability of Dual-Phase 980/1180 Steel Grades, JOM, Vol. 70, pp. 918-923, DOI: 10.1007/s11837-018-2852-x.
[26] Cheah, L.W. 2010. Cars on a Diet: The Material and Energy Impacts of Passenger Vehicle Weight Reduction in the U.S. PhD Thesis, The Engineering Systems Division, Massachusetts Institute of Technology.